TECHNICAL MEMORANDUM

319

Alternative implementations of the semi-Lagrangian semi-implicit schemes in the ECMWF model

M.J.P. Cullen

Research Department

October 2000

European Centre for Medium-Range Weather Forecasts
Europäisches Zentrum für mittelfristige Wettervorhersage
Centre européen pour les prévisions météorologiques à moyen

Abstract

An important issue for the future development of global models is the degree of implicit solution required for optimum performance, and whether this will change the relative cost-effectiveness of spectral and finite-difference models. This is explored by using a predictor-corrector integration scheme in the ECMWF model, where both steps are integrated using the current semi-implicit procedure. This is equivalent to taking a first iteration towards a fully implicit scheme, using the existing semi-implicit method as a preconditioner. The results show that benefit can be obtained provided that both the nonlinear part of the gravity wave terms and the semi-Lagrangian trajectory are recalculated. This suggests that more fully implicit schemes will be beneficial in numerical models. However, the cost of elliptic solvers will not dominate as significant recalculation of tendencies will be required at each iteration. Another strategic issue is the robustness of semi-Lagrangian schemes at high resolution. These are the only advection schemes that preserve monotonicity that are available for spectral models. As resolution is increased, solutions of the equations always contain motions with the wind direction varying rapidly along the trajectory. These are typically not well treated at current operational resolutions, but limit the time-step that can be used with semi-Lagrangian schemes. We illustrate the effect of selective damping of these motions, which may be desirable until much higher resolutions are reached.

1 Introduction

In the last 20 years, most operational forecast and climate global models have used the spectral technique. This is because of the avoidance of the pole problem, and the ability to implement semi-implicit integration schemes easily, and thus allow higher resolutions to be used for a given amount of computer time. At very low resolutions, the extra accuracy of the spectral method for advection is also important. However, at operational forecast resolutions, the semi-Lagrangian method has usually replaced the spectral method for the advection calculations for reasons of efficiency and the ability to enforce monotonicity constraints. The spectral method is then only used for the history-carrying representation of the dynamical variables, the semi-implicit calculations, and any horizontal diffusion that is required. As the resolution of operational global models is increased further, it is necessary to reassess the case for the spectral method. This is partly because of the increasing cost of the Legendre transforms, but also because the effectiveness of the usual semi-implicit method may be reduced as the problem becomes less uniform in space, and local accuracy more important. This paper concentrates on the latter issue, and assesses the benefits of a more completely implicit treatment of the equations.

Another important issue as resolution is increased is the ability to continue to use a semi-Lagrangian time-step with a maximum Courant number substantially greater than unity. Internal inertio-gravity waves occur in the atmosphere at frequencies greater than the inertial frequency, which is now well resolved, and will form part of the correct solution. However, such motions often have a fast Lagrangian time-scale. The use of large time steps is then dangerous because the conditions on the smoothness of the trajectory may be violated. Since only a limited part of the inertio-gravity wave spectrum can be resolved, it is unlikely that these waves will be predicted accurately. It is therefore undesirable to allow them to restrict model time-steps. We assess the use of selective filtering of motions with a fast Lagrangian time-scale.

These issues are examined using the current version of the ECMWF model. This model is part of the IFS (Integrated Forecasting System) developed jointly with Meteo-France. The ECMWF implementation uses a two-time-level semi-Lagrangian semi-implicit scheme, Temperton et al. (2001). Such schemes are widely used because they give advantages in efficiency, but can suffer from the inherent instability of a forward extrapolation. The stability problems have now been overcome in a satisfactory way for operational use using the SETTLS extrapolation, Hortal (1999). However, the nonlinear terms have to be interpolated to the departure points using linear interpolation, and a very

stable reference state (an isothermal atmosphere at 350 K) had to be introduced for the semi-implicit calculations when the model was extended through the stratosphere. Monotone advection of most quantities is used, and was found to remove the spurious over-activity of the model when the resolution was increased to T213. Since then, tests up to T639 resolution have shown no recurrence of the problem. We can thus expect the use of monotone advection to remain necessary at still higher resolutions.

We first explore whether a more implicit scheme would benefit the accuracy of the model. A more implicit scheme is almost certainly required for the stability of a non-hydrostatic formulation. For instance, the existing non-hydrostatic formulation developed by Meteo-France for the limited area version of the IFS, Bubnova et al. (1995), requires the use of some iteration in the implicit solution procedure. The Canadian GEM model, Cote et al. (1998), achieves a more stable algorithm by using a fully-implicit form of the equations and then solving iteratively using a standard constant-coefficient elliptic solver at each step. This allows second order accuracy in time to be achieved without the SETTLS extrapolation. We show that it also allows the compromise of using linear interpolation of the nonlinear terms at the departure point to be withdrawn. We compare the accuracy of the current scheme with a single iteration of the Canadian scheme. In such a scheme, the competitiveness of the spectral method will depend on how much recalculation is required between each call to the implicit solver. An extreme case would be that all the calculations have to be repeated, in which case the proportion of the cost in the implicit solver will be unaffected. If only a few terms have to be recalculated, the cost of the implicit solver, and hence the spectral transforms, will dominate.

We then explore whether the cost-effective use of semi-Lagrangian methods at high resolution will be impeded by the presence of inertio-gravity waves, which have flow directions varying rapidly along the trajectory. We illustrate that the solutions can be stabilised without loss of large scale accuracy by decentering the terms representing gravity waves along the trajectory, providing that the semi-implicit formulation is written in incremental form. The horizontal part of the trajectory computation is not decentered, so that the geostrophic part of the potential vorticity advection is treated with second order accuracy. Though the operational ECMWF scheme is not written in incremental form, to economise on memory, the incremental form is widely used in other models, for instance in the paper of Bubnova et al. (1995) and in the GEM model. A similar form of decentering is used in the GEM model, though none of the trajectory computation is decentered. Decentering is shown to increase robustness by removing oscillations in strong stratospheric jets, and also substantially reduces the amplitude of orographic gravity waves. Large scale scores are improved compared with the control forecast, though some of the extra accuracy gained by the iteration is lost. Tests on extreme synoptic events show that there is some smoothing of synoptic forecasts near the limits of predictability and model resolution.

2 Formulation of the semi-implicit semi-Lagrangian scheme

The basic three-time-level semi-Lagrangian scheme used by ECMWF is described by Ritchie et al. (1995). The two-time-level version is described in Temperton et al. (2001). Satisfactory behaviour of the latter was achieved by modifying the surface pressure and thermodynamic equations to reduce spurious responses to orography, and by using linear interpolation to calculate all quantities except the basic flow variables at the departure points. Further improvements were obtained by the second order extrapolation in time (SETTLS) introduced by Hortal (1999).

2.1 Iterative improvement of the solution

Following Simmons and Temperton (1997) and Temperton (1997), the semi-implicit equations for a single zonal wavenumber can be written

$$\begin{aligned} \zeta^{t+\Delta t} &= \zeta^t - \Delta t(\mathrm{Z} + \alpha\omega D^{t+\Delta t}) \\ T^{t+\Delta t} &= T^t - \Delta t(\mathrm{T} + \alpha\tau_r D^{t+\Delta t}) \\ p_{surf}^{t+\Delta t} &= p_{surf}^t - \Delta t(\mathrm{P} + \alpha\nu D^{t+\Delta t}) \\ D^{t+\Delta t} &= D^t + \Delta t\left(\mathrm{D} - \alpha(\nabla^2(\gamma_r T + \sigma_r p_{surf}) - \omega\zeta)^{t+\Delta t}\right) \end{aligned} \tag{1}$$

The scheme is written using a general time averaging controlled by a parameter $\alpha : 0 \leq \alpha \leq 1$. $\alpha = \frac{1}{2}$ corresponds to a second order implicit scheme, $\alpha = 1$ to a backward implicit scheme. The other Greek letters denote matrices of values at model levels, and in the case of ω, values at different zonal wavenumbers. The Roman letters denote known quantities. In the operational scheme, these are calculated using the SETTLS extrapolation to achieve second order accuracy in time. The suffices r on the matrices indicates that they are derived from a reference state. No reference state quantities appear in ν and ω. Equations (1) reduce to a single Helmholz equation for the divergence of the form

$$\begin{aligned} D^{t+\Delta t} &= D^t + \Delta t(\mathrm{D} - \alpha\nabla^2(\gamma_r T + \sigma_r p_{surf}) + \omega\zeta)^t \\ &+\alpha^2\Delta t^2\left(\nabla^2(\gamma_r\tau_r + \sigma_r\nu)D^{t+\Delta t} - \omega^2 D^{t+\Delta t} + \mathrm{G}\right) \end{aligned} \tag{2}$$

G represents a combination of the known values Z,P and T.

We first rewrite (1) in the incremental form

$$\begin{aligned} \zeta' &= -\Delta t(\mathrm{Z}_1 + \alpha\omega D') \\ T' &= -\Delta t(\mathrm{T}_1 + \alpha\tau_r D') \\ p'_{surf} &= -\Delta t(\mathrm{P}_1 + \alpha\nu D') \\ D' &= \Delta t\left(\mathrm{D}_1 - \alpha(\nabla^2(\gamma_r T' + \sigma_r p'_{surf}) - \omega\zeta')\right) \end{aligned} \tag{3}$$

where primed quantities are the differences between values at time $t + \Delta t$ and time t, and the 'known' values are modified appropriately as indicated by the suffix by setting $\mathrm{Z}_1 = \mathrm{Z} + \alpha\omega D^t$, with similar definitions of T_1, P_1 and D_1. Equations (3) lead to a Helmholz equation for D'

$$\begin{aligned} D' &= \Delta t(\mathrm{D}_1 + \alpha\Delta t\nabla^2(\gamma_r \mathrm{T}_1 + \sigma_r \mathrm{P}_1) + \omega \mathrm{Z}_1)) \\ &+\alpha^2\Delta t^2\left(\nabla^2(\gamma_r\tau_r + \sigma_r\nu) - \omega^2\right) D' \end{aligned} \tag{4}$$

of identical form to (2). T', ζ' and p'_{surf} are then found using (3). Use of this formulation is slightly more expensive in memory, but gives the same answers as the operational scheme.

We can now test the effect of a more implicit treatment of the gravity wave terms by performing a second iteration. The explicit terms $\mathrm{Z}_1, \mathrm{T}_1, \mathrm{P}_1$ and D_1 are modified by setting

$$\begin{aligned} \mathrm{Z}_2 &= \mathrm{Z}_1 + \alpha\omega D' \\ \mathrm{T}_2 &= \mathrm{T}_1 + \alpha\tau_r D' \\ \mathrm{P}_2 &= \mathrm{P}_1 + \alpha\nu D' \\ \mathrm{D}_2 &= \mathrm{D}_1 - \alpha\Delta t(\nabla^2(\gamma_r T' + \sigma_r p'_{surf}) + \omega\zeta') \end{aligned} \tag{5}$$

We then write the second iteration to (1) as

$$\begin{aligned} \zeta'' &= -\Delta t(\mathrm{Z}_2 + \alpha\omega D'') \\ T'' &= -\Delta t(\mathrm{T}_2 + \alpha\tau_r D'') \\ p''_{surf} &= -\Delta t(\mathrm{P}_2 + \alpha\nu D'') \\ D'' &= \Delta t\left(\mathrm{D}_2 - \alpha(\nabla^2(\gamma_r T'' + \sigma_r p''_{surf}) - \omega\zeta'')\right) \end{aligned} \tag{6}$$

and form a Helmholz equation for a second correction to the divergence.

$$\begin{aligned} D'' = \Delta t\left(\mathrm{D}_2 + \alpha\Delta t(\nabla^2(\gamma_r \mathrm{T}_2 + \sigma_r \mathrm{P}_2) + \omega Z_2)\right) \\ +\alpha^2\Delta t^2\left(\nabla^2(\gamma_r\tau_r + \sigma_r\nu_r) - \omega^2\right) D'' \end{aligned} \tag{7}$$

The remaining fields are then updated using (6).

In the next experiment, we test the effect of also recalculating the semi-Lagrangian trajectory. The equations for predicting the departure point in the first and second iterations are

$$\begin{aligned} x^*_a &= x_d + \frac{1}{2}(u_d + u_a) \\ y^*_a &= y_d + \frac{1}{2}(v_d + v_a) \\ z^*_a &= z_d + (1-\alpha)w_d + \alpha w_a \\ x_a &= x_d + \frac{1}{2}(u_d + (u+u')_a) \\ y_a &= y_d + \frac{1}{2}(v_d + (v+v')_a) \\ z_a &= z_d + (1-\alpha)w_d + \alpha(w+w')_a \end{aligned} \tag{8}$$

where u', v', w' are derived from (3). Using (8), we obtain new estimates Z^*, T^*, P^*, D^* for the explicit terms Z_1, T_1, P_1, D_1 etc. These are used instead of Z_2, T_2, P_2, D_2 in (6) to calculate the second iteration of the prognostic variables.

This scheme is an iterative approximation to a centred trapezoidal fully implicit scheme, using the existing semi-implicit scheme as a preconditioner. Note that the horizontal trajectory calculation is never decentered. This is to ensure that the geostrophic potential vorticity advection is treated with second order accuracy. However, the vertical trajectory calculation, which determines the vertical advection, is treated as a gravity wave term and optionally decentered. No decentering of the trajectory is included in the GEM model scheme. The resulting structure is similar to that of a semi-geostrophic model in which departures from geostrophic balance are damped, but geostrophic advection is treated as accurately as possible. Decentering in an operational model at T319 resolution will damp motions with a Lagrangian frequency comparable to the model time-step (20 minutes). Complete filtering of inertio-gravity waves requires filtering of all motions with a Lagrangian frequency greater than f^{-1}, about 3 hours in middle latitudes (Shutts and Cullen, 1987). This is not easily achievable by this method, nor would it be consistent with the assumed time-averaging scale of the model.

Note also that only a first order accurate approximation is used in the predictor step. This is sufficient to ensure second order accuracy of the complete scheme, and makes each time-step self-contained. Gospodinov (private communication) has shown in simple test problems that using higher order accuracy in the predictor step gives no further benefit.

2.2 Error analysis

We demonstrate the extra accuracy of the iterated scheme over the extrapolated scheme by a linear analysis. Because of the iteration, the multi-level analysis of Simmons and Temperton (1997) is very difficult to carry out. We therefore analyse an equation set with a single vertical mode.

The equations analysed are

$$\begin{aligned} \frac{\partial D}{\partial t} + \nabla^2 \phi = 0 \\ \frac{\partial \phi}{\partial t} + c^2 D = 0 \end{aligned} \tag{9}$$

We assume a spectral discretisation in space, and analyse a single wavenumber with ϕ, D proportional to e^{ikx}. Assume that the effect of the predictor step is to multiply ϕ, D by a complex amplification factor λ^* and that the effect of the complete predictor-corrector step to multiply ϕ, D by a complex amplification factor λ. We assume that the implicit calculation can only be applied to a reference value c_0 of the gravity wave speed c, with the remainder treated explicitly. Then λ^* can be determined from the equations

$$\begin{aligned} (\lambda^* - 1)D - \frac{1}{2}k^2 \Delta t(\lambda^* + 1)\phi = 0 \\ (\lambda^* - 1)\phi + (c^2 - c_0^2)\Delta t D + \frac{1}{2}c_0(\lambda^* + 1)\Delta t D = 0 \end{aligned} \tag{10}$$

giving

$$\begin{aligned} \lambda^*(1 + \frac{1}{4}c_0^2 k^2 \Delta t^2) = (1 + \frac{1}{4}(c_0^2 - 2c^2)k^2 \Delta t^2) \pm \\ \sqrt{\left(\frac{1}{2}(c_0^2 - 3c^2)k^2 \Delta t^2 + \frac{1}{8}(c_0^2 - 2c^2)(c_0^2 - c^2)k^4 \Delta t^4\right)} \end{aligned} \tag{11}$$

A similar calculation for the corrector step leads to a quadratic equation for λ in terms of λ^*

$$\begin{aligned} \lambda^2(1 + \frac{1}{4}c_0^2 k^2 \Delta t^2) + 2\lambda(-1 + \frac{1}{4}c_0^2 k^2 \Delta t^2 + \frac{1}{8}(c^2 - c_0^2)(\lambda^* + 1)k^2 \Delta t^2) + \\ (1 + \frac{1}{4}(c^2 + \lambda^*(c^2 - c_0^2)k^2 \Delta t^2) = 0 \end{aligned} \tag{12}$$

Equations (11) and (12) have to be solved numerically. The modulus of the amplification factor and the relative phase speed are shown in Fig.1 for various choices of c and c_0. There are four values for λ for each choice of c and c_0. The largest modulus and largest phase speed error are plotted.

We compare the results with the analysis of the standard second order extrapolation scheme. This has an amplification factor λ given by the equations

$$\begin{aligned} (\lambda - 1)D - \frac{1}{2}k^2 \Delta t(\lambda + 1)\phi = 0 \\ \lambda(\lambda - 1)\phi + \frac{1}{2}(c^2 - c_0^2)(3\lambda - 1)\Delta t D + \frac{1}{2}c_0^2(\lambda + 1)\Delta t D = 0 \end{aligned} \tag{13}$$

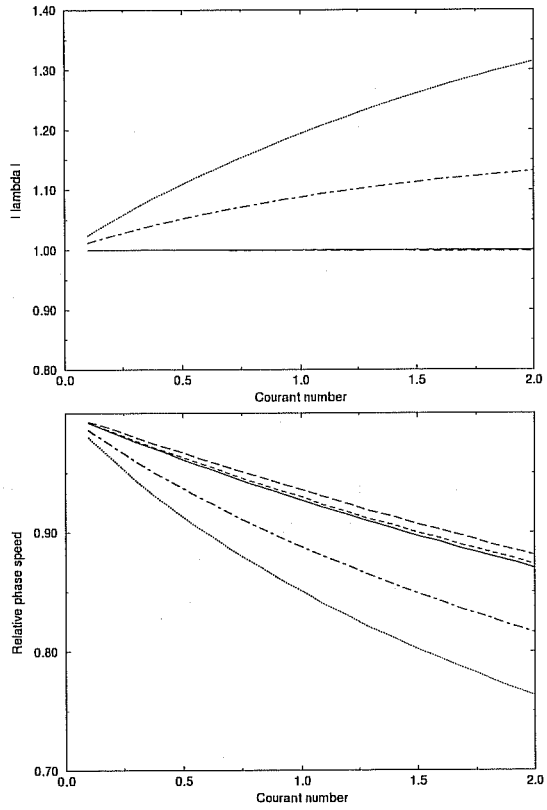

Figure 1. Modulus of the amplification factor and relative phase speed for the predictor-corrector scheme, plotted against Courant number based on actual wave speed. Separate curves represent different choices of reference state with dotted, dash-dotted, solid, dashed and long-dashed lines representing $c_0/c = 0.5, 0.75, 1.0, 1.25, 1.5$.

Both schemes are stable if $c \leq c_0$, as expected from the analysis of Simmons et al. (1978). The schemes perform identically if $c = c_0$. This is because there is no explicit term to extrapolate or iterate in this case. If $c < c_0$ the iterated scheme is much more accurate both in terms of reduced damping and in accuracy of phase speed. In particular, there is much less variation of relative phase speed with c/c_0, and thus less risk of numerical dispersion. The iterated scheme is more unstable for $c > c_0$ than the extrapolated scheme.

We illustrate the effect of decentering in the predictor-corrector scheme by analysing the extreme case $\alpha = 1$. Equations (11) and (12) become

$$\lambda^*(1 + c_0^2 k^2 \Delta t^2) = (1 + \frac{1}{2}(c_0^2 - c^2)k^2\Delta t^2) \pm \sqrt{\left(\frac{1}{4}(c_0^2 - c^2)^2 k^4 \Delta t^4 - c^2 k^2 \Delta t^2\right)} \tag{14}$$

and

$$\lambda^2(1 + c_0^2 k^2 \Delta t^2) + 2\lambda(-1 + \frac{1}{2}(c^2 - c_0^2)k^2\Delta t^2 \lambda^*) + 1 = 0 \tag{15}$$

The amplification factor and relative phase speed are shown in Fig.3. The scheme is stable for all choices of c_0/c, but quite strongly damping with an e-folding time of about 3 time-steps at unit Courant number.

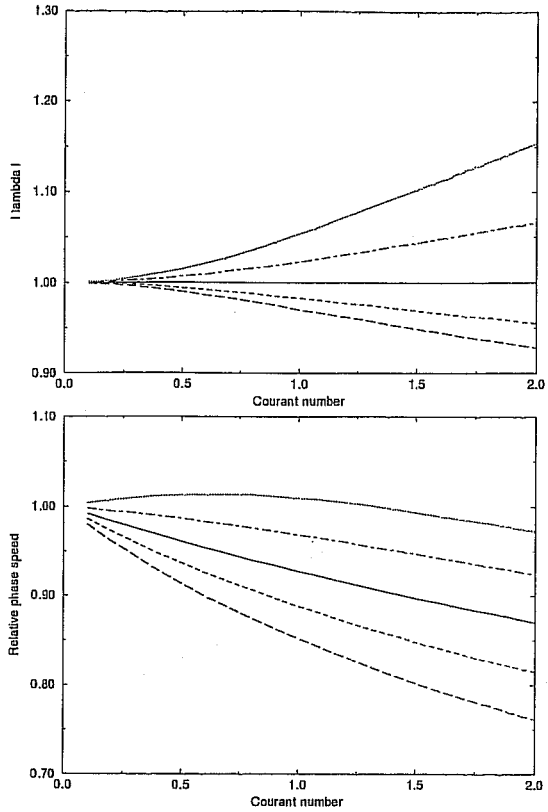

Figure 2. Modulus of the amplification factor and relative phase speed for the extrapolated scheme, notation as Fig.1.

3 Evaluation of the schemes

3.1 Overall statistics

The schemes were tested in two recent versions of the IFS model. Both were run at spectral T319 resolution with a linear transform grid and a 20 minute time-step. The first version used 31 levels, the second used 60 levels with the extra resolution in the stratosphere and planetary boundary layer. The second version also included a trajectory averaging of the physics increments (Wedi (1999)) using extrapolation of the increments from the previous time-level to preserve second order accuracy. In our experiments the decentering applied to the dynamics was therefore for consistency also applied to the physics increments. After initial testing of the robustness of this choice, the linear interpolation of the nonlinear terms at departure points used operationally by ECMWF was replaced by the quasi-monotone cubic scheme used for the interpolation of the model variables themselves. Some improvement in accuracy was found. The overall accuracy of the schemes was then tested by running forecasts from a first set of cases starting from the operational analysis for the 15th of each month of 1998 and using the 31 level model. The more interesting options were then re-tested using the 60 level model and a second set of 14 cases using higher resolution re-analyses. These cases were distributed between August 1998 and December 1999. The standard anomaly correlation and r.m.s scores were computed for each case and averaged over the sets.

The results from the iterated scheme (6-7) were very similar to the control (not shown) in the first set of cases, and so this experiment was not repeated on the second set. When the trajectory was also iterated using (8) there was a noticeable positive impact, which was repeated on the second set of cases. Fig.4 shows the combined results. Note that the improved anomaly correlation is achieved

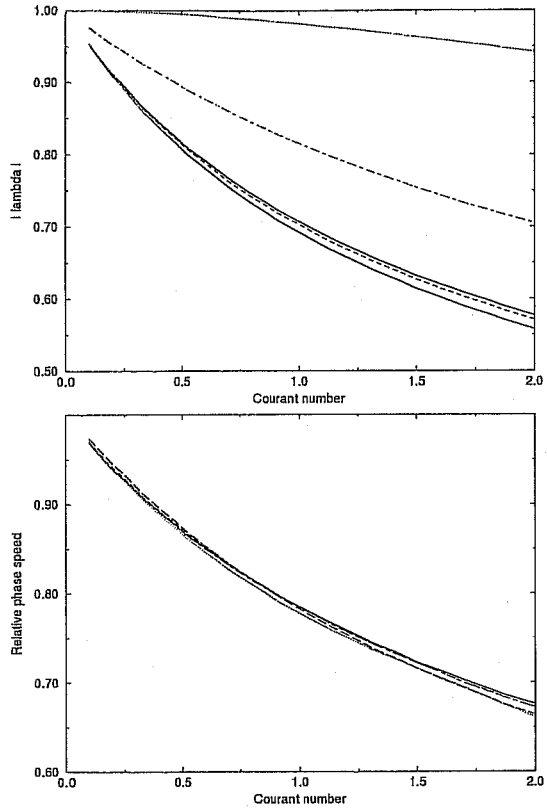

Figure 3. Modulus of the amplification factor and relative phase speed for the extrapolated scheme, notation as Fig.1.

with a very small reduction in r.m.s. error, suggesting that the improvement does not result from a loss in activity of the simulations. These results suggest that a more implicit treatment of only the gravity wave terms is not worth using, but a more implicit calculation of the advection velocity gives useful extra accuracy.

In Fig.5 we illustrate the effect of a decentered implementation of the iterated scheme using $\alpha = 1$. The overall scores are slightly better than the control, but not as good as the time-centred iterated scheme at the point where the forecasts are skillful. At the end of the forecast period the anomaly correlations are better in the decentered integrations, but this is probably because of loss of activity, as illustrated by the reduction in r.m.s. error.

The level of activity and balance in the forecasts is assessed by measuring the the r.m.s. vertical velocity and the standard deviation of the mean sea-level pressure. The former includes both the vertical velocity associated with synoptic motions, and internal gravity waves, the latter reflects the level of synoptic activity. Results are shown in Tables 1 and 2. The control run and both the iterated and decentered schemes have a similar level of vertical velocity. In the decentered scheme, this partly results from a reduction in convective activity and associated increase in resolved vertical motion, particularly in the tropics, which is related to the way the physics is interfaced, rather than to the integration scheme. The iterated scheme gives a slightly lower standard deviation of PMSL. The decentering reduces this further by about 4 percent up to day 5, but rather more after day 5.

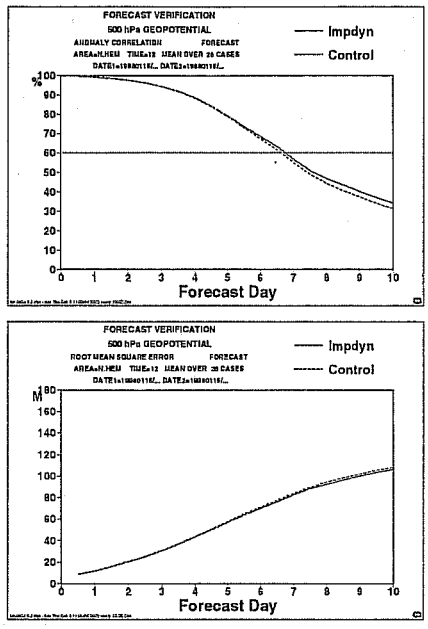

Figure 4. Anomaly correlations (percent) and r.m.s. errors (m) of 500hpa height for 26 test cases. Iterated scheme plotted against the control.

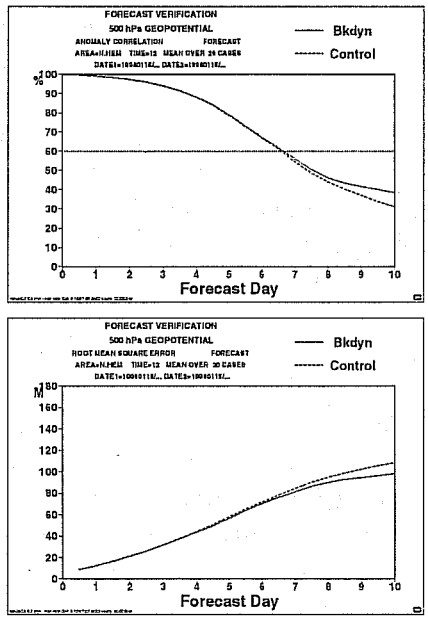

Figure 5. Anomaly correlations (percent) and r.m.s. errors (m) of 500hpa height for 26 test cases. Decentered scheme plotted against the control.

3.2 Results -individual cases

We first illustrate the stabilising effect of the decentering on the trajectories. Fig. 6 shows the winds at level 5 (about 1.15 hpa) for a case in August 1998. The maximum wind strength is about 140 ms^{-1}, so that the Courant number for advection with the 60km grid and 1200s time-step used at T319 resolution is 2.8. Both the control and iterated forecasts show oscillations in the wind direction downstream of South America. These appear to be genuine solutions of the equations since the

TABLE 1. ROOT MEAN SQUARE VERTICAL MOTION (PA S^{-1}), 30-90°N AVERAGED OVER TWO TROPOSPHERIC LEVELS.

Experiment	Day 1	Day 3	Day 5	Day 10
Control	0.133	0.122	0.122	0.122
Iterated	0.129	0.119	0.123	0.121
Decentered	0.128	0.118	0.123	0.122

TABLE 2. STANDARD DEVIATION OF MEAN SEA-LEVEL PRESSURE (HPA), 30-90°N.

Experiment	Day 1	Day 3	Day 5	Day 10
Control	9.32	9.13	9.27	9.07
Iterated	9.13	8.98	9.14	8.84
Decentered	9.08	8.77	8.81	8.27

iterated scheme, which should be more accurate, gives the same result as the control. However, such oscillations can lead to instability of the semi-Lagrangian scheme. This indeed occurred in this case if, for instance, the damping due to the reference state in the semi-implicit scheme was reduced. The decentered integration removes the oscillations, as would be expected, and ensures robustness.

The second illustration (Fig. 7) is of mountain forced gravity waves downstream of Patagonia later in the same forecast as Fig. 6. The westerly winds reached a speed of about 25ms^{-1} in the lower free troposphere, increasing slowly to 35 ms^{-1} at the tropopause and then much more in the stratosphere. The iterated integration gives a rather lower amplitude than the control run (1.2 Pa s^{-1} in vertical velocity as compared with 1.5 Pa s^{-1}). The decentered integration reduces the peak amplitude to 0.9 Pa s^{-1}, but damps the wave away from the mountain much more strongly. These results suggest that there is some contribution of numerical errors to the wave, as indicated by the difference between the control and iterated integrations, and that the decentering removes a substantial part, but not all, of the gravity waves. The wavelength of the waves is about 1300km, and thus the Lagrangian frequency is about 1.2 $10^{-4}s^{-1}$, very close to the inertial period. The analysis of section 2 shows that the e-folding time will be about 5 hours, consistent with the strong damping of the flow away from the mountain. Close to the mountain the wave is continuously forced, so the damping is less effective.

The effect of the iteration and the decentering on extreme weather systems is illustrated in Figs 8 and 9. These were the two violent storms which caused a great deal of damage in France in December 1999. Forecasts of the storms from different analysis times varied a great deal in skill, showing that they were near the limit of predictability with available observations, assimilation methods and models. The first storm was not accurately predicted 48 hours ahead from the analysis used, as seen by comparing Fig. 8a with Figs 8b to d. The iteration has no noticeable effect, and the decentering has only a very small effect on the central pressure, about 1dm. Forecasts of the second storm 84 hours ahead are more sensitive to the model formulation. In the control run the position of the low is hard to define. The iteration has a slightly beneficial effect, and it is now possible to define a low centre. The decentered forecast is less intense, with the low centre undefined and the pressure generally raised by 5dm compared with the control.

4 Discussion

The results from the iterated semi-implicit scheme suggest that more accuracy can be obtained at a given resolution provided the trajectory is recalculated. In a spectral model this means that sig-

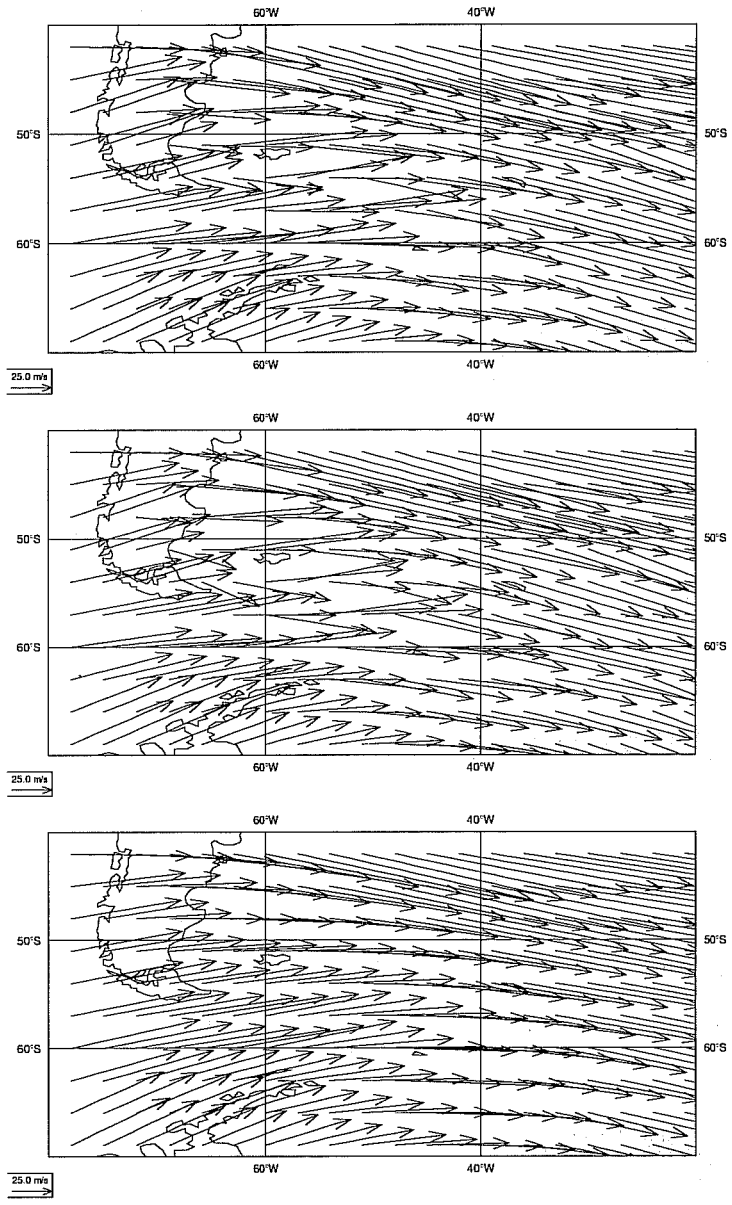

Figure 6. Horizontal winds at level 5 (1.15 hpa) from 24 hour forecasts valid at 1200UTC on 26 August 1998. (a) Control. (b)Iterated scheme. (c) Decentered scheme.

nificant grid-point recalculations are required at each iteration, as well as extra transforms to solve the elliptic problem. Thus the spectral method is still competitive, though the relative cost of the transforms is somewhat increased.

It has also been demonstrated that motions with a fast Lagrangian time-scale which will undermine the robustness of semi-Lagrangian schemes with long time-steps can be filtered with limited impact on synoptic forecasts. However, the motions being filtered are clearly part of the solution, and filtering does not cleanly separate inertio-gravity wave motions from balanced motions since there is not enough frequency separation. Some compromises are inevitable. At the current ECMWF resolution, the performance is sufficiently robust to run without decentering, but this will have to be reviewed at each change of resolution.

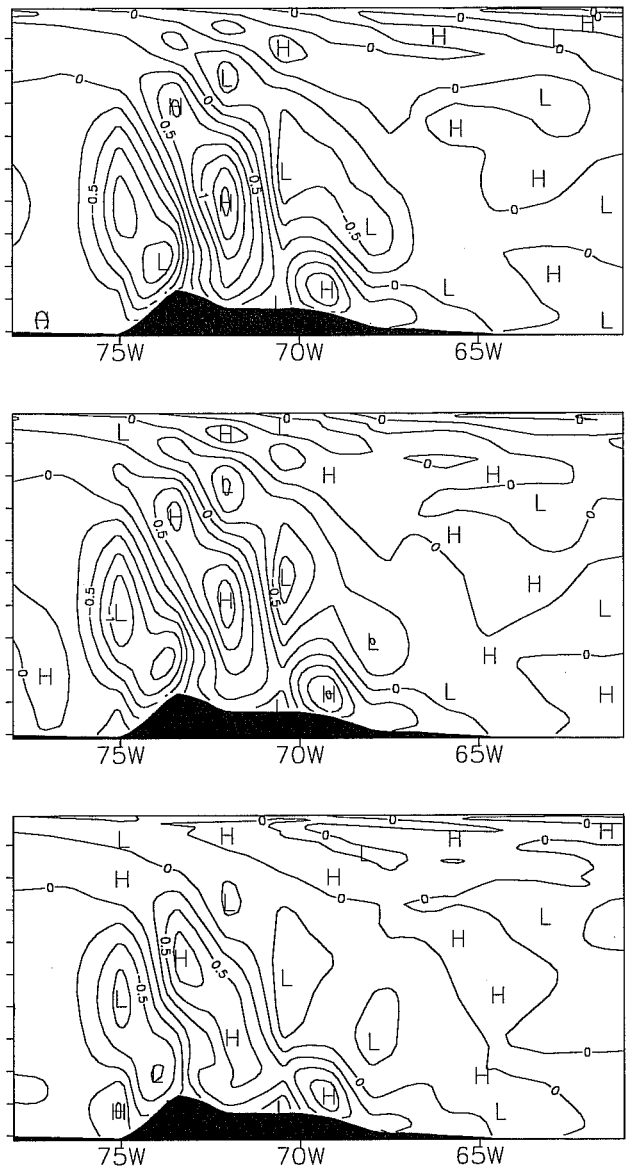

Figure 7. Cross-sections of vertical velocity (Pa s^{-1}) from 53°S78°W to 42°S61°W from 72 hour forecasts valid at 1200UTC on 28 August 1998. (a) Control. (b) Iterated scheme. (c) Decentered scheme.

Further work will examine the potential benefits of iterating the physics as well. This may allow some of the compromises required in the current interfacing (Wedi, 1999) to be avoided. If this is beneficial, it will increase the amount of grid-point recalculation required for each solver iteration. Thus the spectral method will be more competitive than if only the dynamical terms are recalculated.

Acknowledgements

The author wishes to thank the many colleagues at ECMWF, particularly Deborah Salmond, who helped with setting up and running the different versions of the model. He also wishes to thank

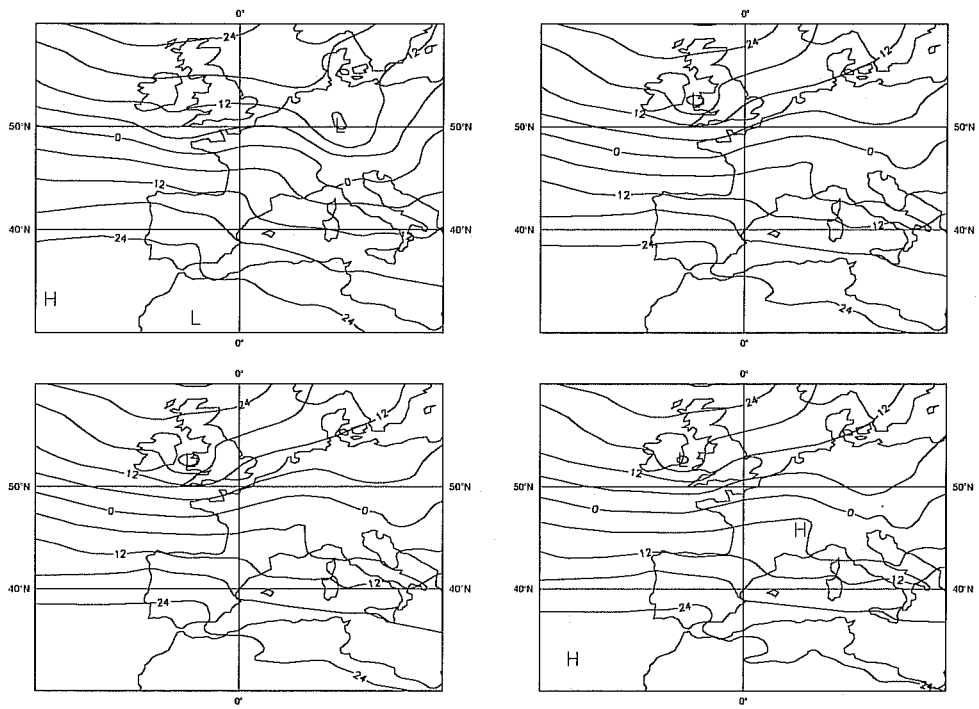

Figure 8. 1000 hpa height from 48 hour forecasts valid at 1200UTC on 26 December 1999. (a) Verifying analysis. (b) Control. (c) Iterated scheme. (d) Decentered scheme.

Mariano Hortal and Clive Temperton (ECMWF), Ilian Gospodinov (Meteo-France) and Andrew Staniforth (UK Met Office) for discussion of the scientific options.

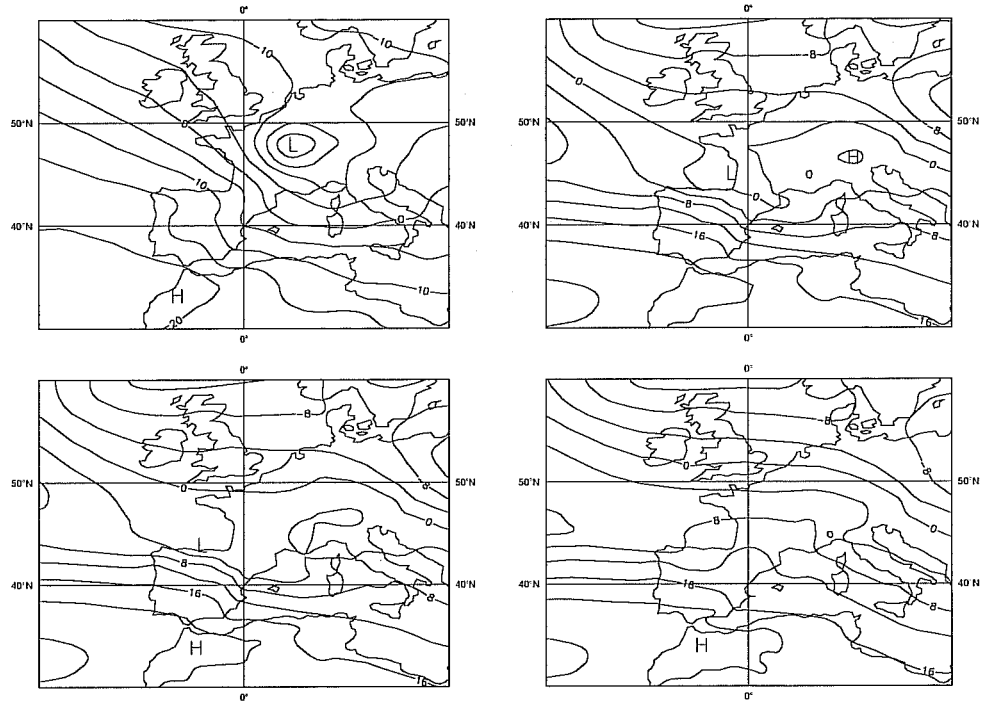

Figure 9. 1000 hpa height from 84 hour forecasts valid at 0000UTC on 28 December 1999. (a) Verifying analysis. (b) Control. (c) Iterated scheme. (d) Decentered scheme.

References

Bubnova, R., Hello. G., Benard, P. and Geleyn, J. -F. Integration of the fully-elastic equations cast in the hydrostatic-pressure terrain-following coordinate in the framework of the ARPEGE/ALADIN NWP system. *Mon. Weather Rev.*, **123**, 515-535, 1995

Bubnova, R., Hello. G., Benard, P. and Geleyn, J. -F. Integration of the fully-elastic equations cast in the hydrostatic-pressure terrain-following coordinate in the framework of the ARPEGE/ALADIN NWP system. *Mon. Weather Rev.*, **123**, 515-535, 1995

Cote, J., Gravel,S. , Mettot, A., Patoine, A., Roch, M. and Staniforth, A. The operational CMC-MRB Global Environmental Multiscale (GEM) Model. Part I. Design consideration and formulation. *Mon. Weather Rev.*, **126**, 1373-1395, 1998

Hortal, M. The development and testing of a new two-time-level semi-Lagrangian scheme (SETTLS) in the ECMWF forecast model. *ECMWF Tech. Memo.*, no. 292, 1999

Ritchie, H., Temperton, C., Simmons, A., Hortal, M., Davies, T., Dent, D. and Hamrud, M. Implementation of the semi-Lagrangian method in a high-resolution version of the ECMWF forecast model. *Mon. Weather Rev.*, **123**,489-514, 1995

Shutts, G. J. and Cullen, M. J. P. Parcel stability and its relation to semi-geostrophic theory. *J. Atmos. Sci.*, **46**, 2684-2697, 1987

Simmons, A. J. Hoskins, B. J. and Burridge, D. M. Stability of the semi-implicit method of time integration. *Mon. Weather Rev.*, **106**, 405-412, 1978

Simmons, A. J. and Temperton, C. Stability of a two-time-level semi-implicit integration scheme for gravity wave motion. *Mon. Weather Rev.*, **125**, 600-615, 1995

Temperton, C. Treatment of the Coriolis terms in semi-Lagrangian spectral models. in 'Numerical Methods in Atmosphere and Ocean Modelling. The Andre Robert Memorial Volume. (C.Lin, R.Laprise, H.Ritchie, Eds.), Canadian Meteorological and Oceanographic Society, Ottawa, Canada, 279-292, 1997

Temperton, C., Hortal, M. and Simmons, A. J. A two-time-level semi-Lagrangian global spectral model. *Quart. J. Roy. Meteorol. Soc.*, **127**, to appear

Wedi, N.P. The numerical coupling of the physical parametrizations to the "dynamical" equations in a forecast model. *ECMWF Tech. Memo.*, no. 274,1999.